

Neuro-fuzzy model of concrete exposed to various regimes combined with De-icing salts

Ahmed Ghazy^{1a} and Mohamed. T. Bassuoni^{*2}

¹Public Works Department, City of Winnipeg, Canada and Department of Civil Engineering, Alexandria University, Egypt

²Department of Civil Engineering, University of Manitoba, Winnipeg, MB, Canada

(Received October 5, 2017, Revised February 8, 2018, Accepted February 9, 2018)

Abstract. Adaptive neuro-fuzzy inference systems (ANFIS) can be efficient in modelling non-linear, complex and ambiguous behavior of cement-based materials undergoing combined damage factors of different forms (physical and chemical). The current work investigates the use of ANFIS to model the behavior (time of failure (TF)) of a wide range of concrete mixtures made with different types of cement (ordinary and portland limestone cement (PLC)) without or with supplementary cementitious materials (SCMs: fly ash and nanosilica) under various exposure regimes with the most widely used chloride-based de-icing salts (individual and combined). The results show that predictions of the ANFIS model were rational and accurate, with marginal errors not exceeding 3%. In addition, sensitivity analyses of physical penetrability (magnitude of intruding chloride) of concrete, amount of aluminate and interground limestone in cement and content of portlandite in the binder showed that the predictive trends of the model had good agreement with experimental results. Thus, this model may be reliably used to project the deterioration of customized concrete mixtures exposed to such aggressive conditions.

Keywords: Neuro-fuzzy systems; concrete, De-icing salts; environmental conditions; durability

1. Introduction

In cold regions, concrete infrastructure (e.g., roads, bridges) are typically exposed to aggressive service conditions due to harsh climates, particularly when combined with de-icing salts. The damage disintegrates the hydrated cement paste to various levels based on the prevailing exposure conditions and key mixture design parameters of concrete (Ghazy and Bassuoni 2017a). Studies on the extent of damage typically classified the problem into physical and chemical natures (Cody *et al.* 1996, Litvan 1976). Physical damage can occur due to a number of processes such as high degree of saturation, crystallization of salt in concrete pores and thermal mismatches during freeze/thaw cycles, while the chemical effects include detrimental reactions between the de-icers and the cement paste or aggravation of expansive aggregate reactions (i.e., alkali-aggregate reactions) (Ghazy and Bassuoni 2017a, Heisig *et al.* 2016, Wang *et al.* 2006).

While enormous efforts have been expended in laboratory and field studies on the physical and chemical mechanisms of damage of concrete, only a few computer-based models have been developed to assist engineers in the prediction of the service life of concrete exposed to harsh environments (e.g., freezing-thawing (F/T) cycles, wetting-drying (W/D) cycles) combined with de-icing salts (Tamimi

et al. 2008). In particular, modeling the transport properties of concrete has received much attention, to indicate the ease of saturation of concrete and in turn its vulnerability to damage (Tamimi *et al.* 2008, Johannesson *et al.* 2003). Despite the significant improvements and sophistication of computer models for the transport processes in concrete, it is still challenging to predict the behavior of concrete exposed to aggressive environments including chemical and physical parameters based only on transport properties. This is due to simplified assumptions in these models such as the saturated condition of concrete and overlooking the effect of environmental conditions (temperature, relative humidity) existing in the field (Marchand *et al.* 2009, Tamimi *et al.* 2008, Johannesson *et al.* 2003). In addition, excluding the chemical interactions in these ions transport models, especially in the presence of de-icing salts, does not reflect the behavior of cementitious materials because the damage process of concrete is dynamically complex due to the dissolution of existing phases (e.g., calcium hydroxide (CH) and calcium silicate hydrate (C-S-H)) and formation of new products (e.g., Kuzel's salts, Friedel's salt, ettringite, gypsum and oxchloride phases), which alter the characteristics of the cementitious paste (Ghazy and Bassuoni 2017a). Recently, multi-ionic modeling approaches have been developed to provide more reliable service-life predictions of the complicated interactions between ions and hydrated cement paste (Marchand *et al.* 2009). However, these approaches may not be easily applicable by transportation agencies as a result of long computational time and/or the complex nature of input data required (i.e., diffusion coefficient, permeability, porosity, moisture isotherm, thermal conductivity and heat capacity, and hydrated cement paste and pore solution compositions).

*Corresponding author, Associate Professor
E-mail: Mohamed.Bassuoni@umanitoba.ca

^aResearch and Standards Intern, Ph.D., EIT
E-mail: Aghazy@winnipeg.ca

For these complex durability issues, which involves physical and chemical interactions, artificial intelligent techniques, such as neural networks (NNs), fuzzy inference systems (FIS), adaptive neuro-fuzzy inference systems (ANFIS), have been promisingly applied in concrete research. Using a well-defined experimental database (input-output), artificial intelligence can be an efficient tool in modeling complex durability issues such as chloride-induced corrosion, alkali aggregate reaction, carbonation depth and sulfate attack of concrete (Cho *et al.* 2016, Tabatabaei *et al.* 2014, Boğa *et al.* 2013, Balasubramaniam *et al.* 2012, Bianchini and Bandini 2010, Bassuoni and Nehdi 2008, Hu and Tang 2006). ANNs are information-processing algorithms, which are composed of a number of interconnected processing elements analogous to neurons resulting in high learning capabilities (Haykin 1999). Comparatively, FIS allows a stochastic data-driven modeling approach, which uses IF-THEN rules and logical operators to establish qualitative relationships among the variables in the model (Ross 2004). Therefore, ANFIS is a hybrid system incorporating the learning abilities of ANNs and semantic knowledge representation and inference capabilities of FIS that have the ability to self-modify their membership functions to achieve a desired performance (Ross 2004, Brown and Harris 1994). It can model the qualitative aspects of human knowledge and reasoning processes without employing precise quantitative analyses. This framework makes ANFIS modeling more systematic and less reliant on expert knowledge.

Hu and Tang (2006) successfully applied ANFIS to evaluate the effect of composition of fly ash on suppressing the expansion of concrete due alkali aggregate reaction. Also, Bassuoni and Nehdi (2008) developed ANFIS models to predict the behavior of a wide range of self-consolidating concrete mixtures under various sodium sulfate exposure regimes. They showed that the sensitivity analyses for such approach had good agreement with experimental results and microstructural analysis. Bianchini and Bandini (2010) applied ANFIS to predict the performance of pavements using the parameters routinely collected by transportation agencies (e.g., the development of distresses on the pavement surface by a rolling wheel deflectometer) to characterize the condition of an existing pavement. Also, Balasubramaniam *et al.* (2012) established an ANFIS model to estimate the performance characteristics of reinforced high-strength concrete beams subjected to different levels of corrosion damage. They concluded that ANFIS can be an alternative approach for the evaluation of degradation as both training and testing data errors were within reasonably small limits ($RMSE \leq 13.7\%$). An ANFIS model had been successfully used for the evaluation of chloride ions permeability in concrete containing blast furnace slag, calcium nitrite-based corrosion inhibitors, and a combination of these components with 92.2% accuracy (Boğa *et al.* 2013). Recently, Cho *et al.* (2016) also proposed ANFIS to estimate the carbonation depth of reinforced concrete members, in which deterioration was reflected based on data obtained from field inspections of nine buildings. They stated that the proposed ANFIS algorithm closely estimated the carbonation depths and provided relatively good accuracy compared to the carbonation depth estimation methods of the Korea

Concrete Institute and the Japan Society of Civil Engineers. Based on the promising use of this approach in modeling complex durability issues of concrete, the present study aims at predicting the time of failure (*TF*) for a variable range of concrete mixtures made with different types of cement without or with supplementary cementitious materials (SCMs: fly ash and nanosilica) under various exposure regimes combined with the most widely used chloride-based de-icing salts (individual and combined) using ANFIS. The ANFIS model was developed, trained, and tested using experimental data from a comprehensive testing program conducted at the University of Manitoba. Full details on the experimental part of this program are beyond the scope of the current study and can be found elsewhere (Ghazy and Bassuoni 2018a, 2018b, Ghazy and Bassuoni 2017a). In the prequalification stage of a construction project, this model can effectively assist in selecting optimum mixtures proposed for a specified exposure.

2. Experimental program

2.1 Materials

The cements used in the experimental program of this study were general use cement (GU) and Portland limestone cement (PLC), which meet CSA A3001 (CSA 2013) specifications; twelve mixtures were prepared, most of which contained SCMs including Type F (low lime) fly ash (designated as F) conforming to CSA A3001 and nanosilica sol (designated as S), as a replacement of the total binder. To achieve a constant workability level (slump of 50 to 75 mm) for all mixtures, a high-range water reducing admixture, based on polycarboxylic acid and complying with ASTM C494 (2016) Type F, was used at dosages in the range of 50 to 400 ml/100 kg of the binder. In addition, an air-entraining admixture was used to obtain a fresh air content of $6 \pm 1\%$. Locally available natural gravel (max. size of 9.5 mm) was used as a coarse aggregate; its specific gravity and absorption were 2.65 and 2%, respectively. The fine aggregate was well-graded river sand with a specific gravity, absorption, and fineness modulus of 2.53, 1.5% and 2.9, respectively. The water-to-binder ratio (*w/b*) and total binder content for all mixtures were kept constant at 0.40 and 400 kg/m^3 , respectively. Single binder (control) mixtures were prepared from 100% GU cement, representing typical concrete pavements in North America, or PLC. Fly ash was used to prepare blended binders with GU and PLC cements without or with nanosilica, at dosages of 20% and 30% by the total binder content (i.e., 80 and 120 kg/m^3 , respectively). Finally, the nanosilica was added at a single dosage of 6% by the total binder content (i.e., solid content of 24 kg/m^3), as a replacement of the cement component in the binder, to prepare binary (comprising GU or PLC and nanosilica) and ternary binders (comprising GU or PLC cements, fly ash and nanosilica). This dosage of nanosilica sol was found to advantageously affect the fresh and hardened properties of cementitious materials (Ghazy *et al.* 2016, Said *et al.* 2012). Table 1 shows the mixture design proportions of the concrete tested in this program.

Table 1 Proportions of mixtures per cubic meter of concrete

| Mixture ID. | Cement (kg/m ³) | Fly Ash (kg/m ³) | Nanosilica (kg/m ³) | Water ^a (kg/m ³) | Coarse Aggregate (kg/m ³) | Fine Aggregate (kg/m ³) |
|------------------|-----------------------------|------------------------------|---------------------------------|---|---------------------------------------|-------------------------------------|
| <u>GU group</u> | | | | | | |
| GU | 400 | -- | -- | 160 | 1096 | 590 |
| GUF20 | 320 | 80 | -- | 160 | 1077 | 580 |
| GUF30 | 280 | 120 | -- | 160 | 1068 | 575 |
| GUS | 376 | -- | 48 | 136 | 1091 | 587 |
| GUF20S | 296 | 80 | 48 | 136 | 1072 | 577 |
| GUF30S | 256 | 120 | 48 | 136 | 1063 | 573 |
| <u>PLC group</u> | | | | | | |
| PLC | 400 | -- | -- | 160 | 1096 | 590 |
| PLCF20 | 320 | 80 | -- | 160 | 1077 | 580 |
| PLCF30 | 280 | 120 | -- | 160 | 1068 | 575 |
| PLCS | 376 | -- | 48 | 136 | 1091 | 587 |
| PLCF20S | 296 | 80 | 48 | 136 | 1072 | 577 |
| PLCF30S | 256 | 120 | 48 | 136 | 1063 | 573 |

^aAdjusted amount of water considering the water content of nanosilica (aqueous solution with 50% solid content of SiO₂)

Sodium chloride (NaCl), dihydrate form of calcium chloride (CaCl₂·2H₂O) and hexahydrate form of magnesium chloride (MgCl₂·6H₂O) with purity of 99, 96 and 96%, respectively were used to prepare the salt solutions. In addition, combined salts (MgCl₂·6H₂O and CaCl₂·2H₂O) were applied to simulate anti-icing and de-icing strategies. Different concentrations were used in these studies, as shown in Table 2. These concentrations had been selected to maintain similar ionic concentration of chloride (Cl⁻) ions in each solution for each state.

2.2 Experimental procedures

Constituent materials were mixed in a mechanical mixer and cast in prismatic molds (50×50×285 mm) to prepare triplicates for each mixture. Also, four replicates cylinders (100×200 mm) were prepared in order to evaluate the penetrability of the concrete specimens according to ASTM C1202 (2012). The specimens were demoulded after 24 h and then cured up to 28 days at standard conditions (22±2°C and 98% RH) according to ASTM C192 (2016). Recent studies have shown that the addition of nanosilica in concrete, even in mixtures containing 30% fly ash, accelerates the rate of hydration and microstructural development to a level comparable to concrete prepared from single binders containing 100% ordinary cement (Ghazy *et al.* 2016, Said *et al.* 2012). Hence, the curing period was kept constant to provide a uniform basis of comparison among all mixtures.

To evaluate the durability of the tested mixtures to the chloride-based de-icing salts (individual and combined) when combined with different environmental conditions, four exposure regimes were adopted:

- Exposure I is a continuous immersion exposure in which prismatic specimens were fully immersed in the high concentration solutions (Table 2) of various de-icing salts at 5°C up to 540 days. The solutions were

Table 2 Concentration of de-icing salt solutions

| Type of Salt | Moderate Concentration | | | High Concentration | | |
|--------------------------------------|-----------------------------|--------------------------------|---|-----------------------------|--------------------------------|---|
| | Salt Concentration Mass (%) | Chloride Concentration (mol/l) | Chloride Concentration ^a (ppm) | Salt Concentration Mass (%) | Chloride Concentration (mol/l) | Chloride Concentration ^a (ppm) |
| NaCl | 14.2 | 2.83 | 100,630 | 23.3 | 4.52 | 160,071 |
| MgCl ₂ | 11.9 | 2.82 | 100,735 | 19.1 | 4.52 | 160,069 |
| CaCl ₂ | 13.6 | 2.81 | 100,731 | 21.9 | 4.51 | 160,067 |
| MgCl ₂ +CaCl ₂ | 5.9+6.8 | 2.82 | 100,733 | 9.6+10.9 | 4.52 | 160,073 |

^aThe ionic concentration of Cl⁻ ions in each solution was verified by ion chromatography according to ASTM D 4327 (2011).

renewed every two weeks to keep a continual supply of de-icing salts, thus providing aggravated damage conditions.

- Exposure II is a wetting/drying (W/D) exposure in which prismatic concrete specimens were subjected to wetting in the high concentration solutions (Table 2) followed by drying. A W/D cycle (five days) consisted of full immersion of specimens for two days in the de-icing salt solutions at a temperature of 5°C, followed by drying at 23±2°C and 55±5% RH for two days and an additional day at 40±2°C and 30±5% RH in an environmental chamber. This cyclic exposure might mimic the consecutive built up of Cl⁻ ions within concrete surface from winter and wet spring conditions followed by drying periods during summer. The solutions were also renewed every two weeks and this exposure continued for 540 days (108 cycles).

- Exposure III is a freezing/thawing (F/T) exposure according to the general procedures of ASTM C666 test procedure A, expect that de-icing solutions were used instead of water and the frequency of F/T cycles per day was less to allow chemical reactions, if any. The duration of one F/T cycle was 12 hours: freezing at -18±1°C for 7 h and thawing at 4±1°C for 3.5 h, and 45 min. to ramp to the minimum freezing temperature or the maximum thawing temperature. Moderate and high concentrations (Table 2) were used in this exposure to cover two different states (solution with and without ice) according to the phase diagrams for these salts (Kelting 2010). The solutions were renewed every two weeks and the exposure continued for 540 days (1080 cycles).

- Exposure IV is a combination of W/D followed by F/T procedures to mimic the field performance of concrete pavements (successive spring/summer and winter seasons, respectively). A spring/summer season was simulated by 6 W/D cycles similar to exposure III, while a winter season was composed of 30 successive F/T cycles similar to exposure IV with moderate concentration solutions. This regime of exposure has been applied for 540 days (i.e., 12 spring/summer alternating with 12 winter seasons).

Before any exposure, the initial physico-mechanical properties of the intact specimens were measured. For all

specimens, the initial mass, length (ASTM C 157 (2014)) and dynamic modulus of elasticity, E_d (ASTM C 215 (2014)) were recorded. Specimens were removed from the solutions at specified time intervals (every 2 weeks), and the free expansion of prisms was immediately measured. Subsequently, debris, if any, were removed by a nylon brush, and the specimens were left to dry under $23 \pm 2^\circ\text{C}$ and 50% RH for 30 min before visual inspection and measurement of mass and fundamental transverse frequency. Relative to the initial values, the changes in mass, length and dynamic modulus of elasticity (RE_d) versus time of exposure were calculated.

In order to evaluate the physical resistance (penetrability) of the concrete specimens, the rapid chloride permeability test (RCPT) was performed according to ASTM C1202 (2012). To alleviate the effects of electrolysis bias and temperatures on the trends, the penetration depth of chloride ions/front into concrete, which better correlates to the physical characteristics of the pore structure, was determined (Bassuoni and Nehdi 2006). Following the RCPT, the discs were axially split and sprayed with 0.1 M silver nitrate solution which forms a white precipitate of silver chloride, to measure the average physical penetration depth of chloride ions. The average depth was determined at five different locations along the diameter of each half specimen. This depth is considered to be an indication of the ease of ingress of external fluids, and thus the continuity of microstructure.

3. ANFIS model

3.1 Database

The database for training and testing the model developed herein comprised 480 data points from 12 mixtures (Table 1) that were exposed to four de-icing salt solutions with different concentrations under four exposure regimes (full immersion at 5°C , W/D, F/T, and cyclic W/D alternating with F/T). The experimental results revealed that the resistance of concrete exposed to these environments combined with de-icing salts is a function of physical penetrability (magnitude of intruding chloride), aluminate content in cement and content of portlandite available for chemical reactions in the hydrated paste. Also, the interground limestone content in PLC contributed to improving the resistance of concrete to de-icing salts due to synergistic physical and chemical actions of limestone in the matrix. Therefore, the model and database had input variables to cover both physical and chemical parameters: penetration depth of chloride ions, interground limestone content, aluminate content (C_3A), and portlandite content at 28 days (before exposure), as well as the type and concentration of the de-icing salt and code of environmental exposure. The latter code was arbitrarily assigned with numbers from 1 to 4 to designate the sequence of experiments (Table 3), and it does not implicate the weight or aggression level of a specific exposure. The TF was the determined experimental parameter in the database and hence the predicted output of the model. Currently, there is no failure limit for evaluating the resistance of concrete

Table 3 Coding of exposure regimes

| Description of Exposure | Designated Code |
|-------------------------------------|-----------------|
| Full immersion at 5°C | I |
| Wetting/Drying (W/D) | II |
| Freezing/Thawing (F/T) | III |
| Cyclic W/D alternating with F/T | IV |

Table 4 Range of training and testing the time of failure (TF)

| Training Data | | | Testing Data | | |
|---------------|------|------|--------------|------|------|
| Min. | Max. | Avg. | Min. | Max. | Avg. |
| 45 | 540 | 463 | 45 | 540 | 446 |

exposed to de-icing salts under different environmental conditions. Therefore, in this paper, the TF was determined based on an increase in expansion beyond 0.25%, considerable mass loss (more than 20%), decline in RE_d below 60%, and/or breakage of specimens by transverse macro-cracks as each of these criteria were observed to present complete disintegration or failure of the specimens. 345 data points of the data set were randomly assigned to the training set, while the remaining (135) data points was employed for testing the model's performance. The properties of the training and testing data for the model are listed in Table 4. The average expansion, mass loss, and RE_d (failure limits) for the minimum TF (45 days; Table 4) were 2.8%, 25%, and 45%, respectively, while these limits were 0.02%, 0.05%, and 98% for the maximum TF (540 days).

3.2 Approach for developing the ANFIS model

3.2.1 Clustering

The ANFIS model was developed in MATLAB environment (2016). Subtractive fuzzy clustering was generated to establish rule-based relationships among the input and output parameters. The data was divided into clusters to generate the fuzzy inference system. Subtractive clustering was used to initialize the ANFIS model instead of grid partitioning due to the large number of input parameters that might have led to an excessive number of rules which makes the calculations of the ANFIS network extremely slow and perhaps without convergence of the global error. Clustering methods convert a universe of data into homogenous groups classified according to cluster centers from which the distance of data points is computed (Brown and Harris 1994). This method considers that each data point can act as a candidate for the center of clusters; thus, a density measure, D_i , at data point x_i is defined as

$$D_i = \sum_{j=1}^n \exp\left(-\frac{\|x_i - x_j\|^2}{(r_a)^2}\right) \quad (1)$$

where, a is a collection of n data points $\{x_1, x_2, x_3, \dots, x_i\}$ in an M -dimensional space, r_a is the radius of cluster, and $(x_i$ and $x_j)$ are data vectors in the data space including both input and output dimensions. A data point will have a high-density value if it has many neighboring data points. In

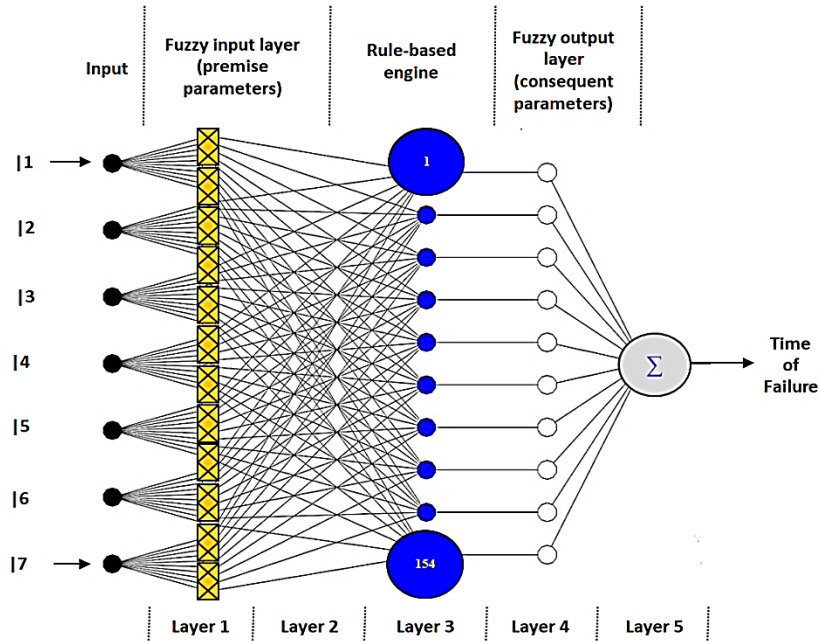


Fig. 1 Architecture of the ANFIS model. (Note: |1: interground limestone content, |2: C₃A content, |3: penetration depth of chloride ions, |4: portlandite content |5: type of de-icing salt, |6: concentration of de-icing salt, |7: code of environmental exposure)

contrast, data points outside the r_a contribute only slightly to the density measure.

After the density measure of each data point had been calculated, the data point with the highest density measure was selected as the first cluster center. Then, the density measure for the next cluster center had been revised as follows

$$D_i = D_i - D_i \exp\left(-\frac{\|x_i - x_{cj}\|^2}{\left(\frac{r_b}{2}\right)^2}\right) \quad (2)$$

where, r_b is a positive constant that is relatively greater than the r_a by the squash factor (η), which is a positive constant greater than 1 to avoid closely spaced cluster centers. Once the density calculation for each data point was revised, the next cluster center was selected and so on. This process was repeated until a sufficient number of cluster centers had been generated. The acceptance of a cluster center based on the density value was determined according to an acceptance threshold (ε) and rejection threshold ($\hat{\varepsilon}$). The process continued until all possible clusters in the input-output spaces were found. The number of clusters defines the number of membership functions in the input-output space. Subtractive clustering has four parameters (acceptance threshold (ε), rejection threshold ($\hat{\varepsilon}$), the radius of cluster (r_a), and the squash factor (η) affecting the resultant number of rules for an ANFIS model. In the present study, these values were selected as 0.5, 0.15, 0.5 and 1.25, respectively, as these values led to small numbers of rules and satisfactory performance of the ANFIS model as will be shown later in the text.

3.2.2 Fuzzy inference method

The Sugeno inference method was used in the present study to develop the ANFIS model as this method was

reported to be particularly effective for ANFIS models with given input-output data sets (Ross 2004). For a first-order Sugeno fuzzy model, a typical rule set with two fuzzy IF-THEN conditions can be expressed as

$$\text{Rule}_1: \text{IF } x \text{ is } A_1 \text{ and } y \text{ is } B_1 \\ \text{THEN } z_1 = p_1x + q_1y + r_1 \quad (3)$$

$$\text{Rule}_2: \text{IF } x \text{ is } A_2 \text{ and } y \text{ is } B_2 \\ \text{THEN } z_2 = p_2x + q_2y + r_2 \quad (4)$$

where, A_i and B_i are the fuzzy sets in the antecedent, and p_i , q_i , and r_i are the design parameters which are determined during the training process. The overall output (z) was obtained by a weighted average defuzzification method as follow

$$z = \frac{\sum_{i=1}^N z_i \cdot w_i}{\sum_{i=1}^N w_i} \quad (5)$$

where, N is the number of rules, z_i is the output of the i^{th} rule, and w_i is the weight (consequent) of the i^{th} rule.

3.2.3 Process

Referring to Fig. 1, the ANFIS architecture had five layers. The first and fourth layers contained an adaptive node, while the other layers contained a fixed node. A brief description of each layer is as follows:

- **Layer 1:** Each node (i) generates a membership function of a linguistic category (high, medium, low). The outputs from this layer are the fuzzy membership grade of the inputs, which are given by the following equations

$$Q_i^1 = \mu_{A_i}(x) \quad (6)$$

where, x is the input to node i , and $\mu_{A_i}(x)$ is the

membership function (which can be triangular, trapezoidal, gaussian functions or other shapes) of the linguistic label A_i associated with this node and Q_i is the degree of match to which the input x satisfies the quantifier A_i . Gaussian membership functions are the most popular shape for specifying the fuzzy set because of their smoothness and concise notation (e.g., Cho *et al.* 2016, Boža *et al.* 2013, Bianchini and Bandini 2010, Bassuoni and Nehdi 2008). Therefore, this function was utilized in the current study, as expressed by

$$\mu_{A_i}(x) = \exp\left[-\left(\frac{x-v_i}{2\sigma_i}\right)^2\right] \quad (7)$$

where, v_i and σ_i are the parameters defining the shape of the membership function (premise parameters).

- **Layer 2:** Every node multiplies the input signals from layer 1, and represents the rule nodes and the output Q_i^2 that represents the firing strength of a rule and is computed as

$$Q_i^2 = w_i = \mu_{A_i}(x) \cdot \mu_{B_i}(y) \quad : \quad i = 1,2 \quad (8)$$

- **Layer 3:** The i^{th} node of this layer calculates the ratio of the i^{th} rule's firing strength to the sum of all rules' firing strengths

$$Q_i^3 = \bar{W}_i = \frac{w_i}{\sum_{j=1}^n w_j} \quad : \quad i = 1,2 \quad (9)$$

where, \bar{W}_i represents the normalized firing strengths.

- **Layer 4:** Every node i is a linear function and the coefficients of the function are adapted through a combination of least squares approximation and back-propagation of the form

$$Q_i^4 = \bar{W}_i \cdot z_i = \bar{W}_i \cdot (p_i x + q_i y + r_i) \quad (10)$$

where, p_i, q_i and r_i are a set of consequent parameters of rule i . Thus, the components of the fuzzy rules (premise and consequent parameters) in the rule-based engine are constantly changing at each training epoch until a minimum root mean-squared error (RMSE; 0.05 in the present study) or desired number of epochs (1000 in the present study) is reached.

- **Layer 5:** The result of this layer is obtained as a summation of the outputs of the nodes of the defuzzification layer to produce the overall ANFIS output as shown in Eq. (5).

3.3 Model's description

ANFIS was developed to predict the TF for concrete under various exposure regimes combined with different de-icing salts from the seven input parameters. For the training database, subtractive clustering was applied to the 345 data sets which led to producing 154 fuzzy membership functions for the seven input variables and consequently 154 rules in the rule-based engine were generated. As mentioned previously, the Gaussian membership function was selected, and first-order Sugeno model was adopted as the fuzzy inference method. In the rule-based engine, the fuzzified input variables were connected by T-norm (logical "and") with a minimization operator. The hybrid learning algorithm of the ANFIS combined the gradient method with

the least-square and back-propagation techniques to optimize the membership functions and the parameters. At each epoch, an error measure, usually defined as the sum of the squared difference between actual and desired output, was reduced. Training stopped when either the predefined epoch number or a stable error decrement was obtained. In the current study, the number of iterations (training) continued until a stable error decrement (after 288 epochs) was observed. Finally, defuzzification of the output (TF) was done by the weighted average method, as described earlier.

4. Results and discussion

After successful training, testing data (not included in the training data) were applied to gauge the ANFIS predictions for unknown data, and thus its generalization. The performance of the ANFIS model was assessed based on the variance accounted for (VAF), average absolute error (AAE) and root mean square error (RMSE) according to the following equations, respectively

$$\text{VAF} = \left(1 - \frac{\text{var}(f_i - z_i)}{\text{var}(f_i)}\right) \times 100\% \quad (11)$$

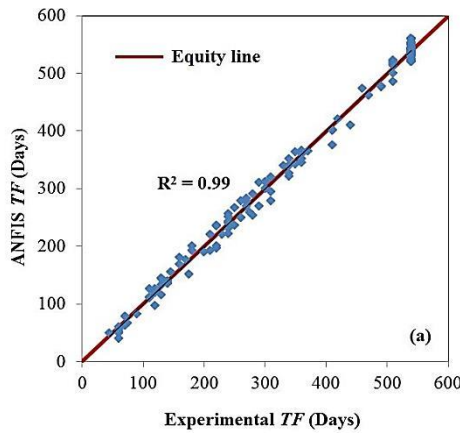
$$\text{AAE} = \frac{1}{n} \sum_{i=1}^n \frac{|f_i - z_i|}{f_i} \times 100 \quad (12)$$

$$\text{RMSE} = \sqrt{\frac{1}{n} \sum_{i=1}^n (f_i - z_i)^2} \quad (13)$$

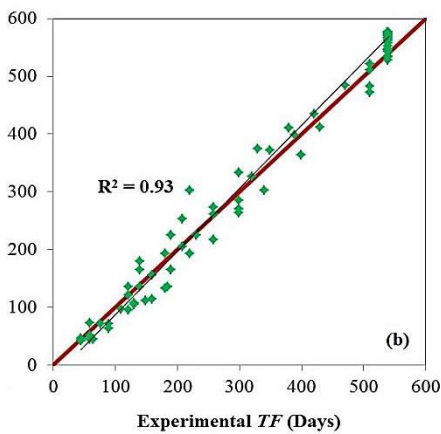
where, f_i and z_i is the measured and predicted values, respectively and n is the number of data points. The higher the VAF, the better the model performance is and vice versa. For instance, a VAF of 100% means that the measured output has been predicted exactly (perfect model). The AAE is defined as the average magnitude of the errors in a set of predictions, which indicates how close the predictions are to the eventual outcomes. Also, the RMSE has a quadratic error rule; as a result, a relatively high weight is given to large errors which are useful when large errors are undesirable in a statistical model. Table 5 summarizes the statistical parameters for the response of the ANFIS model. Also, the ratio of experimental-to-predicted TF for the training and testing data and its coefficient of variation (COV) are tabulated. All these indices indicated that the performance of ANFIS Model was satisfactory. For example, the VAF was 98.7 and 94.3% for the training and testing data, respectively with AAE less than 5%. These trends were substantiated as the ANFIS model reliably captured the input-output relationships since the points are mostly located on or slightly under/above the equity line between the experimental and predicted TF values for the training and testing data, as shown in Fig. 2. The coefficients of determination (R^2) for the training and testing data were 0.99 and 0.93, respectively, indicating strong association between the predicted and experimental TF values. Therefore, it can be deduced that the model has a satisfactory generalization capacity for predicting the TF values of other concrete mixtures exposed to various exposure regimes combined with different types and concentrations of chloride-based de-icing salts (within the range of training data).

Table 5 Performance indices of the ANFIS model

| Training Data | | | | | | Testing Data | | | | | |
|---------------|-------|------|---------------------------------------|------|-------|--------------|-------|------|--|------|-------|
| VAF % | AAE % | RMSE | Average experimental -to-predicted TF | | R^2 | VAF % | AAE % | RMSE | Average of experimental -to-predicted TF | | R^2 |
| | | | Value | COV | | | | | Value | COV | |
| 98.7 | 2.32 | 0.06 | 1.00 | 2.03 | 0.99 | 94.3 | 4.31 | 0.11 | 1.03 | 4.38 | 0.93 |



(a) Training data



(b) Testing data

Fig. 2 Response of ANFIS model in predicting the TF of specimens

5. Effect of the solution type and environmental conditions

In this section, the effect of the solution type on the damage of concrete is evaluated. The overall trends from experimental database and predictions of the ANFIS model in all exposure regimes indicated that the aggression of solutions, in an ascending order, was NaCl, MgCl₂, CaCl₂ and combined (MgCl₂+CaCl₂) salts, as shown in Fig. 3. It can be noted that the combined salt (MgCl₂+CaCl₂) solution, which simulates a synergistic maintenance and protective strategy in winter for concrete pavements and bridges, showed the most severe damage to concrete under all exposures. Thus, this practice should be cautiously reconsidered by transportation agencies.

From the experimental database and predictions of the ANFIS model, it can be noted that the environmental exposure had a pronounced effect on the degree of

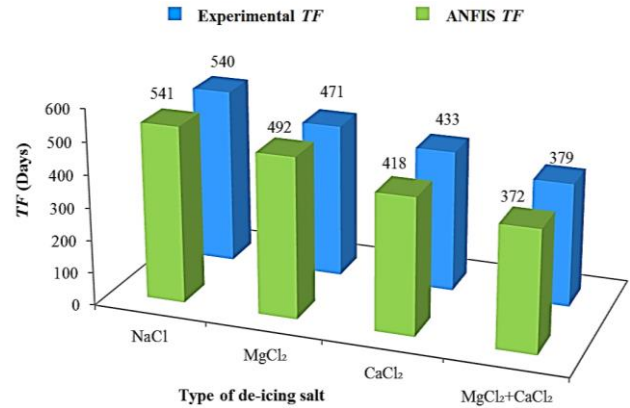


Fig. 3 Average experimental and predicted TF of concrete specimens exposed to different de-icing salts under all the environmental conditions

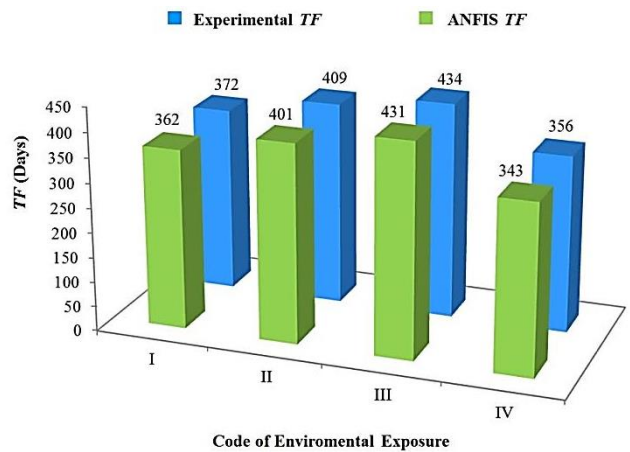


Fig. 4 Average experimental and predicted TF of the specimens exposed to combined salts under all exposure regimes

deterioration of the specimens. Fig. 4, which depicts the average TF of the specimens tested in each exposure under the most aggressive salt solution (combined salts), substantiates this observation. Exposure III (F/T cycles) was the least aggressive (experimental and predicted TF of 434 and 431 days, respectively) relative to the other exposures, while exposure IV (consecutive W/D and F/T cycles), which represents alternating seasonal climatic conditions, was the most aggressive (experimental and predicted TF of 356 and 343 days, respectively). Overall, the results of the four exposure regimes correlated well with their corresponding average predicted TF values. The field-like combined exposure of cyclic environments had additive and perhaps synergistic effects on the specimens, causing the coexistence of complex degradation mechanisms (salt crystallization, surface scaling, frost damage and chemical

Table 6 Levels of the parameters of interest used in the sensitivity analysis

| Parameter of Interest | Variation |
|--|-------------------------------|
| Penetration depth (mm) | 5, 10, 15, 20, 30, 40, 50 |
| Initial portlandite content (J/g) | 5, 10, 15, 20, 30, 40, 50, 60 |
| C ₃ A content (%) | 3, 5, 7, 9, 11 |
| Interground limestone powder in cement (%) | 3, 5, 7, 9, 11, 13, 15 |

degradation) depending on the solution type and concentration as well as the mixtures design variables. Thus, such cyclic environmental conditions should also be considered besides individual testing approaches for developing performance tests that provoke multiple damage mechanisms to improve the understanding of their combined effects on normal and emerging concretes, and hence allow a better modeling of the life-cycle performance of concrete in the field.

6. Sensitivity analyses

The purpose of this section is to investigate the ability of the model to capture the sensitivity of the predicted properties to individual input parameters. The sensitivity analysis was done by fixing all the input parameters except the variable of interest (Table 6) to evaluate its effect within the range of training data. The selected parameters of interest were the physical penetration depth of chloride, initial portlandite content, C₃A content, and interground limestone powder content in the cement. For all the parameters tested, the combined salt (MgCl₂+CaCl₂) solution, which simulates a synergistic maintenance and protective strategy in winter for concrete pavements and bridges, was used as this combination provoked the most severe damage to concrete under all exposure regimes. Also, the combined exposure procedure (alternating W/D with F/T cycles), which mimics field conditions of concrete (successive spring/summer and winter seasons), was implemented in the analysis.

6.1 Sensitivity to physical penetration depth

The sensitivity of the ANFIS model to the penetration depth of chloride ions (physical resistance of concrete to ingress of aggressive fluids) was investigated. For the concrete mixture used in this analysis, the C₃A and interground limestone powder contents were 9 and 4% similar to the GU mixture. Also, the enthalpy of initial portlandite was 63.6 J/g. Fig. 5 shows the ANFIS model predictions of the *TF*. The responses of the model indicated that as the depth of penetration increased, the durability of the specimens decreased. This trend complied with the experimental results as the specimens with smaller whitish precipitate indicating smaller penetration depth of chloride ions in the cross section had better resistance to degradation, which generally performed better and/or survived longer (Ghazy and Bassuoni 2017a). For instance, the binary binder containing nanosilica (GUS) primarily

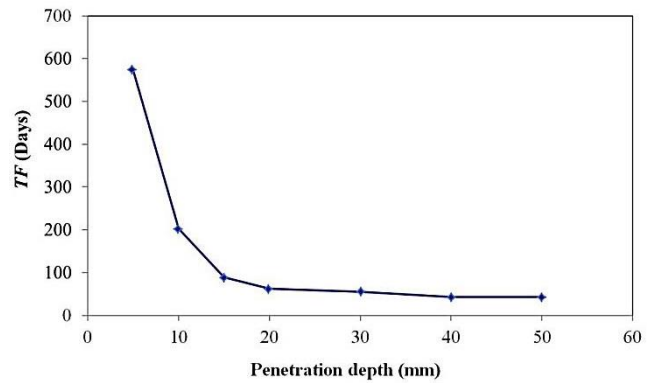


Fig. 5 Sensitivity of the ANFIS model to the penetration depth of chloride ions

resists the degradation due to its significant physical resistance. Using an ultrafine pozzolan such as nanosilica (specific surface of 80,000 m²/kg) in the binary and/or ternary binders produced significantly refined microstructure, and in turn reduced penetrability of these matrices and consequently less solution uptake and less damage (Ghazy and Bassuoni 2017a, Ashok *et al.* 2017). This was clearly captured by the ANFIS model, which showed notable improvement of the *TF* by approximately 160 days when the penetration depth dropped from 50 mm to 10 mm and by more than 500 days when the penetration depth was lower than 10 mm (Fig. 5) when the other parameters were kept constant.

6.2 Sensitivity to initial portlandite content

Portlandite is a key component in the chemical reaction of hydrated paste with de-icing salts, forming complex compounds (oxychloride phases), resulting in chemical degradation of hardened concrete (Ghazy and Bassuoni 2017a, Wang *et al.* 2006, Cody *et al.* 1996). To test the sensitivity of the ANFIS model to the initial portlandite content in the binder (before exposure), the C₃A content, interground limestone powder and physical resistance for the created mixtures were kept constant at 9%, 4% and 20 mm, respectively. Fig. 6 shows the ANFIS model predictions of the *TF*. It can be noted that the model was sensitive to the initial portlandite content in the cementitious matrix, as it showed poor performance (early *TF*) for the mixtures containing high portlandite contents and vice versa. This complies with thermal, mineralogical and microscopy analyses which showed that the degradation of the specimens exposed to de-icing salts under such exposure regimes was mainly controlled by the availability of portlandite with respect to the infiltration of chloride ions in the matrix to stimulate chemical degradation (Ghazy and Bassuoni 2017a). This complies with the experimental observations as the W/D (II) or combined exposures (IV) increased the long-term efficiency of pozzolanic reactivity of Type F fly ash, and thus the better performance of specimens comprising fly ash. In contrast, the long-term activity of fly ash was hindered in binary specimens exposed to continuous immersion at 5°C (exposure I) or F/T cycles (exposure III) as indicated by the

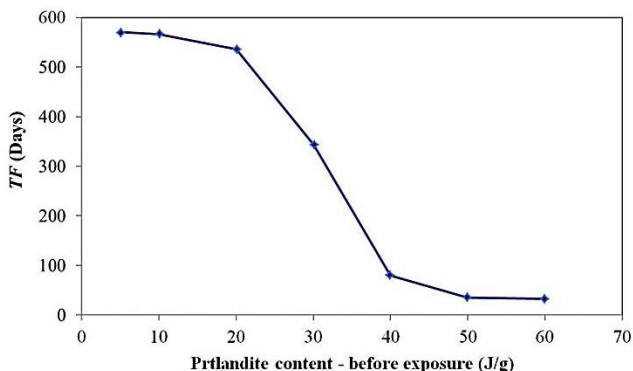


Fig. 6 Sensitivity of the ANFIS model to the initial portlandite content in the binders

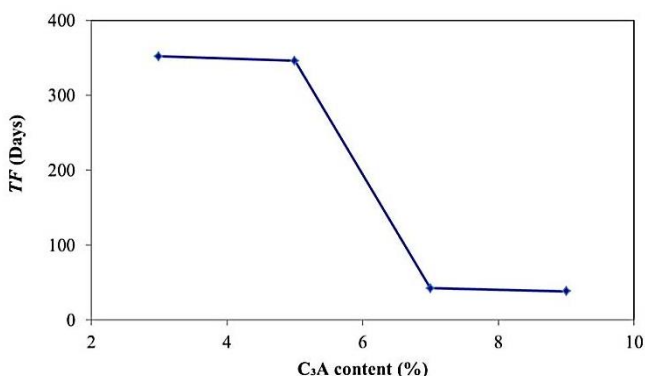


Fig. 7 Sensitivity of the ANFIS model to the C₃A content

abundance of portlandite in these specimens. Hence, the binary fly ash specimens generally failed (but after the GU specimens with higher initial portlandite contents) under regimes I and III. Conversely, nil portlandite content was observed in ternary cementitious systems comprising GU, fly ash and nanosilica, which corresponded to sound mechanical properties and longevity. Using nanosilica with a specific surface of 80,000 m²/kg in the ternary binders led to speeding up the rate of hydration and pozzolanic reactions (fly ash reactivity) which led to significant reduction of the initial portlandite contents (Ghazy *et al.* 2016, Madani *et al.* 2012, Said *et al.* 2012).

6.3 Sensitivity to C₃A content

To test the sensitivity of the ANFIS model to the C₃A content in the binder, the interground limestone powder, initial portlandite content, and physical resistance for the created mixtures were fixed at 4%, 63.6 J/g, and 20 mm, respectively. Fig. 7 shows the predictions of the ANFIS model reflecting the variations in the C₃A content between 3 to 9% (within the range of training data). The responses of the model indicated that as the C₃A content decreased, the durability of the specimens notably improved. This was exhibited by a delay of the TF by more than 300 days when the C₃A content dropped to 5%. This agrees with experimental observations, as the mixtures containing low C₃A content (e.g., PLC specimens) had slower chemical activity and less quantities of the reaction products [calcium oxychloride, Friedel’s salt, ettringite, magnesium

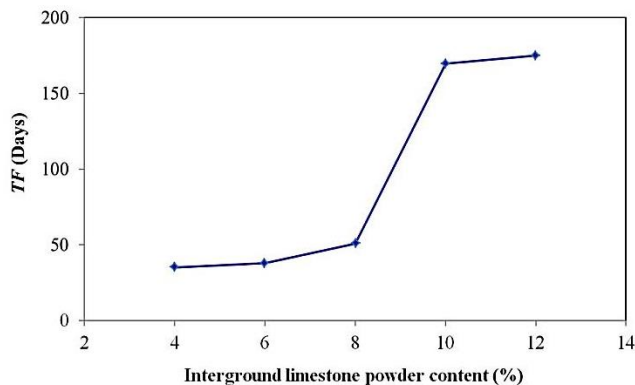


Fig. 8 Sensitivity of the ANFIS model to the interground limestone powder content in cement

oxychloride, and gypsum, irrespective of the type of solution] as observed in the mineralogical analysis (Ghazy and Bassuoni 2017a). Therefore, specimens with low C₃A content in the binder performed better and/or survived longer than the specimens with high C₃A content.

6.4 Sensitivity to limestone content

To examine the effect of variation in interground limestone content in cement on the responses of the ANFIS model, the C₃A content, portlandite content, and physical resistance for the created mixture were fixed at 9%, 63.3 J/g, and 20 mm, respectively. Fig. 8 shows that the prediction of the ANFIS model was relatively sensitive to the transition from low (i.e., 4% in the GU mixtures) to high (i.e., 12% in the PLC mixtures) contents of limestone in the cementitious matrix. This complies with thermal, mineralogical and microscopy analyses which showed that the higher limestone component in PLC mixtures changed the hydration pattern of the binder due to formation of carboaluminate-type compounds rather than other aluminate compounds (e.g., hydroxy-AFm and monosulfate) (Ipavec *et al.* 2013, Lothenbach *et al.* 2008). The ability of carboaluminate phases to bind chloride was reported to be significantly less than other aluminate compounds (Ipavec *et al.* 2013). Subsequently, the system with high interground limestone content had slow chemical activity (limited formation of Friedel’s salt). This chemical effect of limestone explains the notable improvement in the resistance of the mixtures containing high interground limestone content (within the range of training data) exposed to chloride-rich environments, which generally performed better and/or survived longer than the specimens with low interground limestone content as exhibited by a delay of TF by more than 150 days in the ANFIS model (Fig. 8).

7. Conclusions

- The present study showed that adaptive neuro-fuzzy inference systems (ANFIS) can be used to predict the complex behavior of cement-based materials under

combined damage mechanisms. This model integrates the advantages of artificial neural networks (e.g., self-learning and pattern recognition) and fuzzy inference systems (e.g., accommodating uncertainty, linguistic use, and approximation).

- The ANFIS model developed in the present study accurately predicted the time of failure (*TF*) of a wide range of concrete mixture designs under various exposure regimes combined with the most widely used chloride-based de-icing salts (individual and combined). The model had a good generalization capacity beyond the training stage as verified by results obtained on new testing data within the range of training database.

- Predictions of the ANFIS model showed that the combined salt ($MgCl_2+CaCl_2$) solution, which simulates a synergistic maintenance and protective strategy in winter for concrete pavements and bridges, and the field-like combined exposure, which mimics field performance had additive and perhaps synergistic effects on aggravating the degradation of concrete. Thus, this practice should be cautiously reconsidered by transportation agencies, especially with the intensive winter maintenance practices adopted by transportation agencies to cope with climatic changes.

- Sensitivity analyses showed that the developed model captured the effect of individual input parameters on the results. Thus, this model can be used to forecast the deterioration of tailor-made concrete mixtures exposed to such aggressive conditions. In the design and prequalification stage of a construction project, this model can reduce the need for exhaustive trial batches and long-term experiments, thus facilitating decision-making on optimum mixtures.

- The developed ANFIS model is versatile and can be re-trained to encompass wider ranges of input variables, different concentrations of de-icing salt solutions, other types of de-icing salts, other environmental conditions, etc. Once, such data becomes available in the future, the re-training process of this model would be readily achievable.

Acknowledgments

The authors highly appreciate the financial support from Natural Sciences and Engineering Research Council of Canada (RGPIN/4024-2014), University of Manitoba Graduate Fellowship, and City of Winnipeg (317756). The IKO Construction Materials Testing Facility and Manitoba Institute for Materials at the University of Manitoba in which these experiments were conducted have been instrumental to this research.

References

Ashok, M., Parande, A.K. and Jayabalan, P. (2017), "Strength and durability study on cement mortar containing nano materials", *Adv. Nano Res.*, **5**(2), 99-111.
 ASTM C 157 (2014), Standard Test Method for Length Change of Hardened Hydraulic-Cement Mortar and Concrete1, ASTM

International, West Conshohocken, PA, V. 4.02.
 ASTM C 215 (2014), Standard Test Method for Fundamental Transverse, Longitudinal, and Torsional Resonant Frequencies of Concrete Specimens, ASTM International, West Conshohocken, PA, V. 4.02.
 ASTM C1202 (2012), Standard Test Method for Electrical Indication of Concrete's Ability to Resist Chloride Ion Penetration, ASTM International, West Conshohocken, PA, V. 4.02.
 ASTM C192 (2016), Standard Practice for Making and Curing Concrete Test Specimens in the Laboratory, ASTM International, West Conshohocken, PA, V. 4.02.
 ASTM C494 (2016), Standard Specification for Chemical Admixtures for Concrete, ASTM International, West Conshohocken, PA, V. 4.02.
 ASTM D4327 (2011), Standard Test Method for Anions in Water by Suppressed Ion Chromatography, ASTM International, West Conshohocken, PA, V. 11.01.
 Balasubramaniam, V., Raghunath, P.N. and Suguna, K. (2012), "An adaptive neuro-fuzzy inference system based modeling for corrosion-damaged reinforced HSC beams strengthened with external glass fibre reinforced polymer laminates", *J. Comput. Sci.*, **8**(6), 879-890.
 Bassuoni, M.T. and Nehdi, M.L. (2006), "Enhancing the reliability of evaluating chloride ingress in concrete using the ASTM C 1202 rapid chloride penetrability test", *J. ASTM Int.*, **3**(3), 1-13.
 Bassuoni, M.T. and Nehdi, M.L. (2008), "Neuro-fuzzy based prediction of the durability of self-consolidating concrete to various sodium sulfate exposure regimes", *Comput. Concrete*, **5**(6), 573-597.
 Bianchini, A. and Bandini, P. (2010), "Prediction of pavement performance through Neuro-Fuzzy reasoning", *Comput. Aid. Civi. Infra. Eng.*, **25**(1), 39-54.
 Boğa, A.R., Ö ztürk, M. and Topçu, İ.B. (2013), "Using ANN and ANFIS to predict the mechanical and chloride permeability properties of concrete containing GGBFS and CNI", *Compos. B: Eng.*, **45**(1), 688-696.
 Brown, M. and Harris, C. (1994), *Neuro-fuzzy Adaptive Modelling and Control*, 1st Edition, Prentice Hall, New Jersey, USA.
 CAN/CSA-A3001 (2013), Cementitious Materials for Use in Concrete, Canadian Standards Association, CSA, Mississauga, Ontario, Canada.
 Cho, H.C., Ju, H., Oh, J.Y., Lee, K.J., Hahm, K.W. and Kim, K.S. (2016), "Estimation of concrete carbonation depth considering multiple influencing factors on the deterioration of durability for reinforced concrete structures", *Adv. Mater. Sci. Eng.*, **2016**, Article ID 4814609, 18.
 Cody, R.D., Cody, A.M., Spry, P.G. and Gan, G.L. (1996), "Experimental deterioration of highway concrete by chloride deicing salts", *Environ. Eng. Geosci.*, **2**(4), 575-588.
 Ghazy, A. and Bassuoni, M.T. (2017a), "Resistance of concrete to different exposures with chloride-based salts", *Cement Concrete Res.*, **101**, 144-158.
 Ghazy, A. and Bassuoni, M.T. (2018a) "Response of concrete with blended binders and nanosilica to cyclic environments and chloride-based salts", *Mag. Concrete Res.*, 1-14.
 Ghazy, A., Bassuoni, M.T. and Islam, A.K.M.R. (2018b), "Response of concrete with blended binders and nanosilica to freezing-thawing cycles and different concentrations of de-icing salts", *J. Mater. Civil Eng.*, 1-44.
 Ghazy, A., Bassuoni, M.T. and Shalaby, A. (2016), "Nano-modified fly ash concrete: a repair option for concrete pavements", *ACI Mater. J.*, **113**(2), 231-242.
 Haykin, S. (1999), *Neural Networks: A Comprehensive Foundation*, 2nd Edition, Prentice-Hall, New Jersey, USA.
 Heisig, A., Urbonas, L., Beddoe, R.E. and Heinz, D. (2016), "Ingress of NaCl in concrete with alkali reactive aggregate:

- effect on silicon solubility”, *Mater. Struct.*, **49**(10), 4291-4303.
- Hu, M.Y. and Tang, M.S. (2006), “Use of fuzzy neural network to evaluate effect of composition of fly ash in suppressing AAR”, *ACI Mater. J.*, **103**(3), 161-168.
- Ipavec, A., Vuk, T., Gabrovšek, R. and Kaučič, V. (2013), “Chloride binding into hydrated blended cements: The influence of limestone and alkalinity”, *Cement Concrete Compos.*, **48**, 74-85.
- Johannesson, B.F. (2003), “A theoretical model describing diffusion of a mixture of different types of ions in pore solution of concrete coupled to moisture transport”, *Cement Concrete Res.*, **33**, 481-488.
- Kelting, D.L. and Laxon, C.L. (2010), “Review of effects and costs of road de-icing with recommendations for winter road management in the Adirondack Park”, Adirondack Watershed Institute.
- Litvan, G.G. (1976), “Frost action in cement in the presence of deicers”, *Cement Concrete Res.*, **6**(3), 351-356.
- Lothenbach, B., Le Saout, G., Gallucci, E. and Scrivener, K. (2008), “Influence of limestone on the hydration of Portland cements”, *Cement Concrete Res.*, **38**(6), 848-860.
- Madani, H., Bagheri, A. and Parhizkar, T. (2012), “The pozzolanic reactivity of monodispersed nanosilica hydrosols and their influence on the hydration characteristics of Portland cement”, *Cement Concrete Res.*, **42**(12), 1563-1570.
- Marchand, J. and Samson, E. (2009), “Predicting the service-life of concrete structures-Limitations of simplified models”, *Cement Concrete Compos.*, **31**(8), 515-521.
- MATLAB Documentation (2016), *Fuzzy Toolbox User's Guide of MATLAB*, The MathWorks, Inc.
- Ross, T. (2004), *Fuzzy Logic with Engineering Applications*, John Wiley & Sons, UK.
- Said, A.M., Zeidan, M.S., Bassuoni, M.T. and Tian, Y. (2012), “Properties of concrete incorporating nano-silica”, *Concrete Build. Mater.*, **36**, 838-844.
- Song, Z., Jiang, L. and Zhang, Z. (2016), “Chloride diffusion in concrete associated with single, dual and multi cation types”, *Comput. Concrete*, **17**(1), 53-66.
- Tabatabaei, R., Sanjaria, H.R. and Shamsadini, M. (2014), “The use of artificial neural networks in predicting ASR of concrete containing nano-silica”, *Comput. Concrete*, **13**(6), 739-748.
- Tamimi, A.K., Abdalla, J.A. and Sakka, Z.I. (2008), “Prediction of long term chloride diffusion of concrete in harsh environment”, *Constr. Build. Mater.*, **22**, 829-836.
- Wang, K., Nelsen, D.E. and Nixon, W.A. (2006), “Damaging effects of deicing chemicals on concrete materials”, *Cement Concrete Compos.*, **28**(2), 173-188.